

Table I. Maximum Absorbance Wavelengths and Corresponding Molar Absorptivities of Neutral and Electrooxidized Fc-(OEP)Ge-Fc in CH₂Cl₂ Containing 0.1 M TBAP

electrode reactn ^a	absorbing species	λ_{\max} , nm (ϵ , 10 ⁻⁴ cm ⁻¹ M ⁻¹)	
none	Fc-(OEP)Ge-Fc	439 (14.1)	569 (0.6)
1e oxidn	[Fc-(OEP)Ge-Fc] ⁺	435 (8.0)	561 (0.6)
2e oxidn	[Fc-(OEP)Ge-Fc] ²⁺	434 (5.9)	559 (0.9)
3e oxidn	[Fc-(OEP)Ge-ClO ₄] ⁺	408 (6.1)	537 (0.1) 578 (0.04)

^aSee Figure 1.

voltammetric and spectroelectrochemical measurements were carried out at a Pt electrode in dichloromethane (CH₂Cl₂) containing 0.1 M tetrabutylammonium perchlorate (TBAP).

Four reversible oxidations are observed at $E_{1/2} = 0.14, 0.32, 1.32,$ and 1.57 V in CH₂Cl₂ containing 0.1 M TBAP (see Figure 1). The difference between the third and fourth oxidations of Fc-(OEP)Ge-Fc is 0.25 V, which compares to an average separation of 0.29 ± 0.05 V for oxidation of various metalloporphyrins at the porphyrin π ring system.¹⁶ The difference between the first and second oxidation of Fc-(OEP)Ge-Fc is 0.18 V in CH₂Cl₂, and this agrees with separations of 0.17–0.20 V between the two oxidations of Fc-Si(CH₃)₂-Fc,¹³ Fc-Se-Fc,² and Fc-CH₂-Fc.^{2,3} in CH₂Cl₂ or CH₃CN. More importantly, however, the first oxidation of Fc-(OEP)Ge-Fc is shifted negatively by 0.350 V with respect to the Fc/Fc⁺ couple in the same solvent. This is the most negatively shifted oxidation of any ferrocene complex and compares to potentials of -0.04 and +0.07 V vs. Fc/Fc⁺ for the oxidation of Fc-X-Fc, where X = Si(CH₃)¹³ and Se,² respectively.

Electronic absorption spectra of metalloporphyrins are directly influenced by both the axial ligands bound to the central metal and the charge on the porphyrin ring.¹⁷ The electronic absorption spectrum of Fc-(OEP)Ge-Fc (Figure 2a) is typical of a σ -bonded (OEP)Ge(R)₂ complex. This spectrum is virtually identical with that of C₆H₅-(OEP)Ge-C₆H₅ (Figure 2b) but differs from that of C₆H₅-(OEP)Ge-ClO₄ (Figure 2c).

The spectral changes during the first two oxidations of Fc-(OEP)Ge-Fc are shown in Table I and may provide insights into the mechanism of stabilization of singly oxidized Fc-(OEP)Ge-Fc. Apparently, the oxidized ferrocenyl ligand becomes an electron acceptor. This electron-withdrawing effect of the ligand results in a blue shift of the Soret band.¹⁷ The Soret band is further blue-shifted after the second oxidation which generates a second electron-acceptor Fc ligand. Thus, the large decrease in the Soret band intensity after both the first and the second oxidation of Fc-(OEP)Ge-Fc is attributed to a partial delocalization of charge on the a_{1u} and a_{2u} orbitals of the macrocycle. The absorbing species after abstraction of a third electron is assigned as [Fc-(OEP)Ge-ClO₄]⁺, which results from cleavage of one Ge-Fc bond on the longer spectroelectrochemical time scale (2–5 min). The fourth oxidation is beyond the potential window of CH₂Cl₂, and no spectral changes could be monitored in the thin-layer cell.

In summary, Fc-(OEP)Ge-Fc is the most easily oxidized bridged ferrocene complex studied to date and the first bridged ferrocene complex where delocalization of charge on the bridge can be detected. These effects are attributed to the electron-donating ability of the porphyrin macrocycle which facilitates abstraction of the first and second electron from Fc-(OEP)Ge-Fc. Further stabilization and delocalization of charge on the oxidized species are expected to occur if electron-donating substituents are added to the porphyrin macrocycle, and an evaluation of these data should aid in quantitating the changes in spectra.

Finally, it is also significant to note that Fc-(OEP)Ge-Fc is unusually stable toward light and oxygen. This stability and ease of Fc-(OEP)Ge-Fc oxidation may have interesting properties in terms of the compound's ability to undergo intermolecular pho-

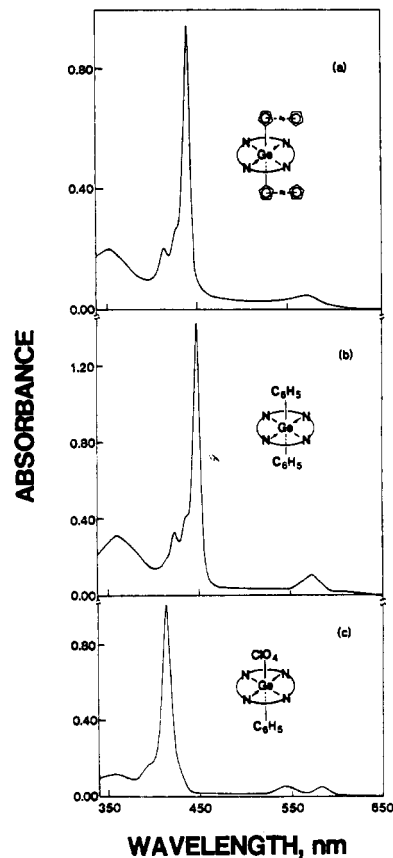


Figure 2. Electronic absorption spectra of (a) Fc-(OEP)Ge-Fc, (b) C₆H₅-(OEP)Ge-C₆H₅ and (c) C₆H₅-(OEP)Ge-ClO₄ in PhCN.

tocatalyzed electron-transfer reactions. This application is now under investigation.

Acknowledgment. The support of the National Science Foundation (Grant Nos. CHE-8515411 and INT-8413696) is gratefully acknowledged.

(18) On leave from the Université de Dijon.

Department of Chemistry
University of Houston
Houston, Texas 77004

K. M. Kadish*
Q. Y. Xu
J.-M. Barbe¹⁸

Received May 21, 1987

Differences in the Band Electronic Structures of the Tetragonal and Orthorhombic Phases of the High-Temperature Superconductor YBa₂Cu₃O_{7-y} (T_c > 90 K)

Sir:

Since the first report¹ of ambient-pressure superconductivity above 90 K in a multiphase sample of the Y-Ba-Cu-O system, a number of studies²⁻¹¹ have been carried out to identify the

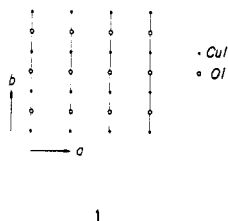
(16) Kadish, K. M. *Prog. Inorg. Chem.* **1986**, *34*, 435.

(17) Gouterman, M. In *The Porphyrins*; Dolphin, D., Ed.; Academic: New York, 1978; Vol. III, pp 1-156.

superconducting phase and determine its structure. From several powder neutron diffraction studies,⁷⁻⁹ it is now known that the Y-Ba-Cu-O phase with the superconducting transition temperature (T_c) greater than 90 K is not tetragonal but orthorhombic, and its composition is $\text{YBa}_2\text{Cu}_3\text{O}_{7-y}$ ($y \approx 0.19$).⁷ X-ray¹⁰ and neutron powder¹¹⁻¹³ diffraction studies show that above 1023 K orthorhombic $\text{YBa}_2\text{Cu}_3\text{O}_{7-y}$ undergoes a reversible phase transition to tetragonal $\text{YBa}_2\text{Cu}_3\text{O}_{7-y}$ ($y \gtrsim 0.5$),¹¹ which can be stabilized at low temperatures by fast quenching.¹²⁻¹⁴ The resulting tetragonal¹⁰⁻¹³ phase appears to exhibit superconductivity at a much lower temperature ($T_c = \sim 50$ K).¹⁰⁻¹⁴ However, it is impossible to state whether or not the tetragonal phase has a ~ 50 K superconducting transition^{10,13,14} and the possibility that this phase is nonsuperconducting cannot be ruled out.^{10,14}

The important structural unit of orthorhombic $\text{YBa}_2\text{Cu}_3\text{O}_{7-y}$ is the $\text{Ba}_2\text{Cu}_3\text{O}_{7-y}^{3-}$ slab, which consists of two CuO_2 layers that sandwich one CuO_3 chain and two Ba^{2+} cations per unit cell (e.g., see Figure 1 of our previous paper¹⁵). In each $\text{Ba}_2\text{Cu}_3\text{O}_{7-y}^{3-}$ slab, the copper atoms (Cu2) of the CuO_2 layers are linked to the copper atoms (Cu1) of the CuO_3 chains via the capping oxygen atoms (O4), thereby forming Cu2-O4-Cu1-O4-Cu2 bridges perpendicular to the slab. The Y^{3+} cations are sandwiched by the $\text{Ba}_2\text{Cu}_3\text{O}_{7-y}^{3-}$ slabs, so that $\text{Ba}_2\text{Cu}_3\text{O}_{7-y}^{3-}$ slabs and layers of Y^{3+} cations alternate along the c axis.

In general, the structure of the tetragonal $\text{YBa}_2\text{Cu}_3\text{O}_{7-y}$ phase is very similar to that of the orthorhombic $\text{YBa}_2\text{Cu}_3\text{O}_{7-y}$ phase. The most important structural difference between the two lies in how the oxygen atoms (O1) are distributed in each plane of the Cu1 atoms. As illustrated in 1, the O1 atoms of the orthorhombic



phase connect the Cu1 atoms along the b axis and together with the capping oxygen atoms O4 form the CuO_3 chains. The tetragonal phase is characterized by a random distribution (disorder) of the O1 atoms between all the Cu1-Cu1 linkages along the a - and b -axis directions. Thus, no infinite CuO_3 chains exist in the tetragonal phase. In the present work, we examine the electronic structure of tetragonal $\text{YBa}_2\text{Cu}_3\text{O}_{7-y}$ by performing tight-binding band calculations^{15,16} on two ordered model structures designed

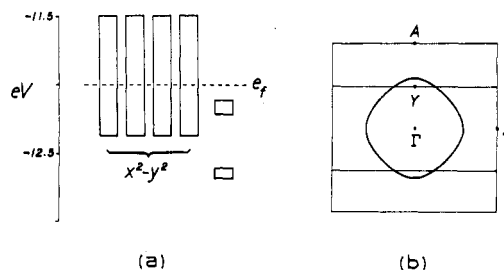


Figure 1. (a) Top six d-block bands calculated for the model 2 of the composition $\text{YBa}_2\text{Cu}_3\text{O}_{6.5}$, where the CuO_2 layer $x^2 - y^2$ bands are each one-fourth filled. (b) Fermi surface associated with each one-fourth-filled $x^2 - y^2$ band, where $\Gamma = (0, 0, 0)$, $X = (a^*/2, 0, 0)$, $Y = (0, b^*/2, 0)$, and $A = (0, b^*, 0)$.

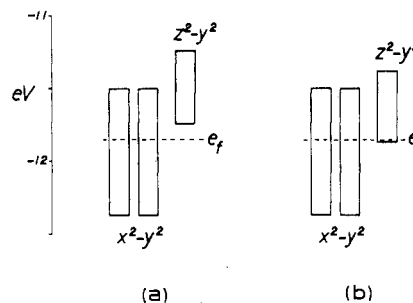
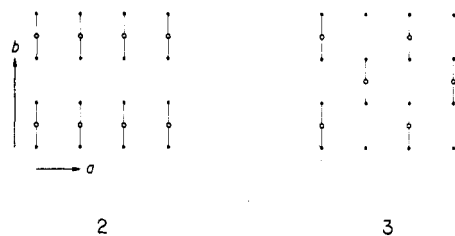


Figure 2. Top three d-block bands calculated for the orthorhombic $\text{YBa}_2\text{Cu}_3\text{O}_7$ phase with the Cu1-O4 distance of (a) 1.850 Å and (b) 1.890 Å. In (a) the CuO_2 layer $x^2 - y^2$ bands are each half-filled, and in (b) they are slightly less than half-filled because the bottom of the CuO_3 chain band is below the Fermi level.

to simulate the tetragonal $\text{YBa}_2\text{Cu}_3\text{O}_{7-y}$ phase and then analyze how the tetragonal and orthorhombic phases differ in their electronic structures.

The single-crystal X-ray diffraction data⁶ of the tetragonal phase are found to accommodate any $\text{YBa}_2\text{Cu}_3\text{O}_{7-y}$ composition with a y value from 0 to 1. However, recent powder neutron diffraction results¹¹ have shown that the orthorhombic to tetragonal phase transition of $\text{YBa}_2\text{Cu}_3\text{O}_{7-y}$ which occurs above 1023 K, is accompanied by the loss of oxygen atoms. Namely, the tetragonal phase is observed when $y \gtrsim 0.5$. It is the O1 atoms that are primarily lost during the orthorhombic to tetragonal phase transition. In the tetragonal phase, the occupation number of the O1 atom sites is close to, but less than, 0.25. Thus, in the present study, we represent the tetragonal $\text{YBa}_2\text{Cu}_3\text{O}_{7-y}$ phases by two ordered structures of composition $\text{YBa}_2\text{Cu}_3\text{O}_{6.5}$ that contain no CuO_3 chains. In 2 and 3 we show two different distributions of



the O1 atoms for the composition $\text{YBa}_2\text{Cu}_3\text{O}_{6.5}$, in which all the Cu1 atoms are equivalent in coordination number and the average occupation number of the O1 atom site is 0.25. These models do not reflect the symmetry of the tetragonal phase but instead try to model the disorder which occurs in that system with ordered supercells. We believe that although these structural models may not exactly reproduce the true shape of the bands associated with the Cu1 atoms, the resultant band widths and band energies will closely reflect those for tetragonal $\text{YBa}_2\text{Cu}_3\text{O}_{7-y}$. It should also be noted that the reported Cu1-O4 distance is slightly shorter

- (5) Syono, Y.; Kikuchi, M.; Oh-ishi, K.; Hiraga, K.; Arai, H.; Matsui, Y.; Kobayashi, N.; Sasaoka, T.; Muto, Y., unpublished results.
- (6) Hazen, R. M.; Finger, L. W.; Angel, R. J.; Prewitz, C. T.; Ross, N. L.; Mao, H. K.; Hadjilacos, C. G.; Hor, P. H.; Meng, R. L.; Chu, C. W. *Phys. Rev. B: Condens. Matter* **1987**, *35*, 7238.
- (7) Beno, M. A.; Soderholm, L.; Capone, D. W., II; Hinks, D. G.; Jorgensen, J. D.; Schuller, I. K.; Segre, C. U.; Zhang, K.; Grace, J. D. *Appl. Phys. Lett.* **1987**, *51*, 57.
- (8) Greedan, J. E.; O'Reilly, A.; Stager, C. V. *Phys. Rev. B: Condens. Matter*, in press.
- (9) Capponi, J. J.; Chaillout, C.; Hewat, A. W.; Lejay, P.; Marezio, M.; Nguyen, N.; Raveau, B.; Soubeyroux, J. L.; Tholence, J. L.; Tournier, R., submitted for publication in *Europhys. Lett.*
- (10) Schuller, I. K.; Hinks, D. G.; Beno, M. A.; Capone, D. W., II; Soderholm, L.; Locquet, J.-P.; Bruynseraede, Y.; Segre, C. U.; Zhang, K., submitted for publication in *Solid State Commun.*
- (11) Jorgensen, J. D.; Beno, M. A.; Hinks, D. G.; Soderholm, L.; Volin, K.; Hitterman, R. L.; Grace, J. D.; Schuller, I. K.; Segre, C. U.; Zhang, K.; Kleefish, M. S., submitted for publication in *Phys. Rev. B: Condens. Matter*.
- (12) Katano, S.; Funahashi, S.; Hatano, T.; Matsushita, A.; Nakamura, K.; Matsumoto, T.; Ogawa, K., private communication.
- (13) Santoro, A.; Miraglia, S.; Beech, F.; Sunshine, S. A.; Murphy, D. W.; Schneemeyer, L. F.; Waszczak, J. V., submitted for publication in *Mater. Res. Bull.*
- (14) Kini, A. M.; Geiser, U.; Kao, H.-C. I.; Carlson, K. D.; Wang, H. H.; Monaghan, M. R.; Williams, J. M. *Inorg. Chem.* **1987**, *26*, 1834.
- (15) Whangbo, M.-H.; Evain, M.; Beno, M. A.; Williams, J. M. *Inorg. Chem.* **1987**, *26*, 1831.

- (16) Whangbo, M.-H.; Evain, M.; Beno, M. A.; Williams, J. M. *Inorg. Chem.* **1987**, *26*, 1832.

in the tetragonal phase than in the orthorhombic phase (i.e., 1.829 (11)¹² and 1.795 (2) Å¹³ in the former phase and 1.850 (3) Å in the latter phase⁷ at room temperature).

Shown schematically in Figure 1a are the top six d-block bands calculated for the model **2** with the Cu1–O4 distance of 1.750 Å,¹⁷ which consist of two narrow d-block bands derived from the Cu1, O1, and O4 atoms and the four wide $x^2 - y^2$ bands derived from the CuO₂ layers. The two Cu1 d-block bands are completely filled, and the four CuO₂ layer $x^2 - y^2$ bands are each one-fourth filled. Therefore, each of the $x^2 - y^2$ bands leads to a closed Fermi surface as shown in Figure 1b. When the Cu1–O4 distance is increased beyond 1.750 Å, the two Cu1 d-block bands are lowered in energy while the CuO₂ layer $x^2 - y^2$ bands remain fixed in energy. Even for the short Cu1–O4 distance of 1.750 Å, the upper Cu1 d-block band is still below the Fermi level by 0.12 eV. Therefore, in tetragonal YBa₂Cu₃O_{7-y} in which the equilibrium Cu1–O4 distance would be close to 1.80 Å at room temperature, any lattice vibrational modes involving the displacements of the O4 atoms are not expected to raise the Cu1 d-block levels above the Fermi level. Our calculations on the model **3** lead essentially to the same results as described above.

Shown in Figure 2a are the top three d-block bands of orthorhombic YBa₂Cu₃O₇ (i.e., a stoichiometric model chosen to represent orthorhombic YBa₂Cu₃O_{7-y}) calculated for its equilibrium structure.¹⁵ The two $x^2 - y^2$ bands of the CuO₂ layers are each half-filled, and the $z^2 - y^2$ band of the CuO₃ chains is empty. It is clear from Figures 1a and 2a that, in the tetragonal phase YBa₂Cu₃O_{7-y} ($y \geq 0.5$),¹¹ the low average coordination number of the Cu1 atoms causes all the d-block levels of the Cu1 atoms to lie either below or near the bottom portion of the CuO₂ layer $x^2 - y^2$ band. In contrast, the orthorhombic phase YBa₂Cu₃O_{7-y} ($y \approx 0.19$)⁷ has one d-block level of each Cu1 atom (i.e., the $z^2 - y^2$ level that forms the $z^2 - y^2$ band of the CuO₃ chains) lying near the top portion of the CuO₂ layer $x^2 - y^2$ band. Consequently, compared with the case for the orthorhombic phases, the tetragonal phase has fewer electrons to fill its $x^2 - y^2$ bands. Thus, each CuO₂ layer $x^2 - y^2$ band is one-fourth filled for the model **2** of YBa₂Cu₃O_{6.5} but half-filled for the orthorhombic YBa₂Cu₃O_{7-y}.¹⁵ In the two-dimensional $x^2 - y^2$ band, the density of states (DOS) peaks at the Fermi level (e_f) for half-filling. Thus, the DOS value at e_f , $n(e_f)$, is substantially smaller for the model **2** of YBa₂Cu₃O_{6.5} than for the orthorhombic YBa₂Cu₃O₇ (i.e., 4.44 vs. 8.85 electrons per three copper atoms per eV). It was found¹⁶ for orthorhombic YBa₂Cu₃O₇ that a slight increase in the Cu1–O4 distance (e.g., from 1.85 to 1.89 Å) lowers the bottom of the CuO₃ chain $z^2 - y^2$ band slightly below the Fermi level as shown in Figure 2b. Thus, certain lattice vibrational modes involving displacement of the O4 atom could cause valence fluctuations of the copper atoms.¹⁶ Since the DOS profile of the CuO₃ chain $z^2 - y^2$ band peaks at the top and the bottom of the band, the $n(e_f)$ value of orthorhombic YBa₂Cu₃O₇ is enhanced greatly as the bottom of the $z^2 - y^2$ band touches the Fermi level, which already occurs near the DOS peak of the CuO₂ layer $x^2 - y^2$ bands.¹⁶ The Ba²⁺ cations may play a vital role in the positioning of the O4 capping oxygen atoms in the Ba₂Cu₃O_{7-y}³⁻ slab and provide a precise spacing between the CuO₃ chains and the CuO₂ layers.

All the special features in the electronic structures of the orthorhombic phase mentioned above arise from the presence of the CuO₃ chains. These special features disappear when the CuO₃ chains are destroyed by partial removal of O1 atoms and random distribution of the remaining O1 atoms in the plane of the Cu1 atoms. Thus, the presence of the CuO₃ chains is essential for the occurrence of high T_c (>90 K) superconductivity in the orthorhombic phase of YBa₂Cu₃O_{7-y}.

We have observed^{15,16,18} that each $x^2 - y^2$ band of the CuO₂ layers in orthorhombic or tetragonal YBa₂Cu₃O_{7-y} is identical in

nature with the $x^2 - y^2$ band of the CuO₄ layers in the superconducting phase La_{2-x}M_xCuO₄ (M = Ba, Sr).¹⁹⁻²⁸ In the latter systems, the T_c value ranges from ~30 to ~40 K for $x \approx 0.15$. In La_{2-x}M_xCuO₄, the occupancy of the $x^2 - y^2$ band is given by $(1 - x)/2$. It has been observed^{19,20} that the T_c value of La_{2-x}M_xCuO₄ sharply drops when $x \geq 0.2$.²⁰ Therefore, it appears that the high T_c superconductivity of La_{2-x}M_xCuO₄ almost disappears when the occupancy of its $x^2 - y^2$ band is less than $x \approx 0.4$. According to this reasoning, the tetragonal YBa₂Cu₃O_{7-y} phase is not likely to be expected to be superconducting since its $x^2 - y^2$ bands are each one-fourth filled.

In view of the possibility that there may exist another phase with a higher T_c (>100 K)²⁹ in the L–Ba–Cu–O system (L = lanthanide), it is important to consider some other possible compositions. The superconducting Ba₂Cu₃O₇³⁻ slab can be thought of as a "single-decker sandwich". An interesting variation of this slab is a multidecker (n -decker) sandwich with n chains and $n + 1$ planes, in which every two adjacent CuO₂ planes sandwich one CuO₃ chain and two Ba²⁺ cations per repeat unit. Such an n -decker sandwich has the formula [Ba_{2n}Cu_{2n+1}O_{5n+2}]⁽ⁿ⁺²⁾⁻. Then a crystal obtained by alternating these n -decker sandwiches with layers of lanthanide ions L³⁺ would have the formula [LBa_{2n}Cu_{2n+1}O_{5n+2}]¹⁻ⁿ. One, therefore, obtains the compositions LBa₂Cu₃O₇, LBa₄Cu₅O₁₂⁻, and LBa₅Cu₆O₁₇²⁻ for $n = 1, 2$, and 3, respectively. Of course, the charges on these n -decker structures may be canceled by an appropriate number of oxygen vacancies. Synthetic efforts toward obtaining such compositions are suggested.³⁰

Acknowledgment. Work at North Carolina State University and Argonne National Laboratory is supported by the U.S. Department of Energy, Office of Basic Energy Sciences, Division of Materials Sciences, under Grant DE-FGO5-86-ER45259 and under Contract W31-109-ENG-38, respectively. We express our appreciation for computing time made available by DOE on the ER-Cray X-MP computer.

- (19) Kanbe, S.; Kishio, K.; Kitazawa, K.; Fueki, K.; Takagi, H.; Tanaka, S. *Chem. Lett.* **1987**, 547.
- (20) Tarascon, J. M.; Greene, L. H.; McKinnon, W. R.; Hull, G. W.; Geballe, T. H. *Science (Washington, D.C.)* **1987**, 235, 1373.
- (21) Bednorz, J. G.; Müller, K. A. *Z. Phys. B: Condens. Matter.* **1986**, 64, 189.
- (22) Bednorz, J. G.; Takashige, M.; Müller, K. A. *Europhys. Lett.* **1987**, 3, 379.
- (23) Takagi, H.; Uchida, S.; Kitazawa, K.; Tanaka, S. *Jpn. J. Appl. Phys., Part 2* **1987**, 26, L123.
- (24) Uchida, S.; Takagi, H.; Kitazawa, K.; Tanaka, S. *Jpn. J. Appl. Phys., Part 2* **1987**, 26, L1.
- (25) Cava, R. J.; van Dover, R. B.; Batlogg, B.; Rietman, E. A. *Phys. Rev. Lett.* **1987**, 58, 408.
- (26) Chu, C. W.; Hor, P. H.; Meng, R. L.; Gao, L.; Huang, Z. J.; Wang, Y. Q. *Phys. Rev. Lett.* **1987**, 58, 405.
- (27) Chu, C. W.; Hor, P. H.; Meng, R. L.; Gao, L.; Huang, Z. J. *Science (Washington, D.C.)* **1987**, 235, 567.
- (28) Jorgensen, J. D.; Schüttler, H.-B.; Hinks, D. G.; Capone, D. W., II; Zhang, K.; Brodsky, M. B.; Scalapino, D. J. *Phys. Rev. Lett.* **1987**, 58, 1024.
- (29) Chen, J. T.; Wenger, L. E.; McEwan, C. J.; Logothetis, E. M. *Phys. Rev. Lett.* **1987**, 58, 1972.
- (30) This paper was presented at the NATO Advanced Research Workshop on Organic and Inorganic Low Dimensional Crystalline Materials, May 3-8, 1987, Menorca, Spain.

Department of Chemistry
North Carolina State University
Raleigh, North Carolina 27695-8204

Myung-Hwan Whangbo*
Michel Evain

Chemistry and Materials Science
Divisions
Argonne National Laboratory
Argonne, Illinois 60439

Mark A. Beno
Urs Geiser
Jack M. Williams*

- (17) Band electronic structure calculations were performed as a function of the Cu1–O4 distance ranging from 1.75 to 1.85 Å. Details of our tight-binding calculations are described in our earlier papers.^{15,16,18}
- (18) Whangbo, M.-H.; Evain, M.; Beno, M. A.; Williams, J. M. *Inorg. Chem.* **1987**, 26, 1829.

Received June 4, 1987